ORIGINAL PAPER

Journal of Anatomy   ANATOMICAL SOCIETY WILEY

Histological differences between lumbar and tail intervertebral discs in mice

Jana Brendler[1] | Karsten Winter[1] | Paul Lochhead[2,3] | Angela Schulz[4] | Albert Markus Ricken[1] (iD)

[1]Institute of Anatomy, Leipzig, Germany

[2]Clinical and Translational Epidemiology Unit, Massachusetts General Hospital and Harvard Medical School, Boston, Massachusetts, USA

[3]Division of Gastroenterology, Massachusetts General Hospital, Boston, Massachusetts, USA

[4]Rudolf-Schönheimer-Institute of Biochemistry, Faculty of Medicine, University of Leipzig, Leipzig, Germany

Correspondence
Albert Markus Ricken, Institute of Anatomy, Liebigstr. 13, DE-04103 Leipzig, Germany.
Email: albert.ricken@medizin.uni-leipzig.de

Abstract

Both the lumbar and tail intervertebral discs (IVD) of mice serve as models for the pathogenesis and histologic progression of degenerative disc disease. Recent studies in mature mice, however, demonstrate that the mechanics and physical attributes of lumbar and tail IVD-endplate (EP)-interfaces are strikingly different. We hypothesized that these structural disparities are associated with differences in the composition and organization of soft tissue elements that influence the biomechanical properties of the spine. Lumbar and tail vertebral segments and discs were collected from the same C57BL/6N and C57BL/6JRj mice, respectively for histological comparison of coronal sections at the ages of 4 weeks (weaned, both strains, C57BL/6N: $n = 7$; C57BL/6JRj: $n = 4$), three (mature, C57BL/6N: $n = 7$; C57BL/6JRj: $n = 4$), twelve (middle aged, C57BL/6JRj only: $n = 3$) and eighteen (old, C57BL/6JRj only: $n = 3$) months old. The histology of lumbar and tail IVD-EP-interfaces of mature mice differed markedly. The lumbar IVD-EP-interphase was characterized by a broad cartilaginous EP, while the tail IVD-EP-interphase comprised a thin layer of cartilage cells adjacent to a broad bony layer abutting the vertebral growth plate. Furthermore, the composition of the nuclei pulposi (NP) of lumbar and tail IVD in mature mice differed greatly. Lumbar NP consisted of a compact cluster of mainly large, uni-vacuolated cells centered in an amorphous matrix, while tail NP were composed of a loose aggregate of vacuolated and non-vacuolated cells. The anuli fibrosi also differed, with more abundant and sharply defined lamellae in tail compared to lumbar discs. The observed histological differences in the EP were even most prominent in weaned mice but were still discernible in middle-aged and old mice. An appreciation of the histological differences between lumbar and tail IVD components in mice, including nucleus pulposus, annulus fibrosus, and endplates, is essential to our understanding of spinal biomechanics in these animals and should inform the design and interpretation of future IVD-studies.

1 | INTRODUCTION

Most vertebrae are separated from each other by intervertebral discs (IVD), which confer flexibility, stability and integrity to the vertebral column (Boszczyk et al., 2001).

Due to the challenges in obtaining tissue from human IVD at different ages or time points in the evolution of IVD disease, animal models have become an invaluable tool for the study of IVD biology (McCann & Séguin, 2016). Mice are frequently used as animal models because of their general characteristics of lower interindividual differences in inbred-mouse strains, short gestation period, large litter sizes, low maintenance costs, availability of species-specific reagents (e.g., antibodies) and the relative ease of genetic and surgical manipulation (Dahia et al., 2009; O'Connell et al., 2007). In addition, mice offer several specific advantages as model for studying IVD aging and degeneration. Mouse lumbar motion segments exhibit mechanical properties and intervertebral disc shapes quite similar to those of humans (Elliott & Sarver, 2004; O'Connell et al., 2007). Furthermore, valuable genetic and surgical models for human disorders associated with degenerative spinal changes already exist, summarized by Alini et al. (2008). Nevertheless, mouse vertebrae differ anatomically from those of humans in several respect and not all biomechanical features of adult human vertebrae, such as multi-axial motion and load transmission, are adequately recapitulated in this animal model (Daly et al., 2016). For example, in contrast to humans, cows, and sheep, mouse IVD retain notochordal cells in their nucleus pulposus throughout much time of their life (McCann & Séguin, 2016). Additionally, mice are quadrupeds and do not normally stand or walk upright on their hindlimbs like humans (McCann & Séguin, 2016).

Mouse tail discs are often preferred in studies over lumbar discs because of their larger size, number, and convenient accessibility (Elliott & Sarver, 2004; Tam et al., 2018). Furthermore, mouse tail discs are easier to manipulate for inducing intervertebral disc degeneration (IDD) in situ. It has recently been demonstrated that mouse lumbar and tail discs differ significantly in gross geometry and mechanical behavior (Elliott & Sarver, 2004; Holguin et al., 2014; O'Connell et al., 2007; Sarver & Elliott, 2005). Physically, mouse tail discs are long in height, with extensive cranial and caudal surface areas, have a rounded transversal plane, and are of almost uniform height in the sagittal plane. In contrast, mouse lumbar discs are short in height, elliptical to kidney-shaped in the transversal plane, and of wedge shape in the sagittal plane (Figure 1, O'Connell et al., 2007). Mechanically, mouse tail discs undergo greater axial displacements, that is, are less stiff than mouse lumbar discs under compression (Sarver & Elliott, 2005).

We hypothesized that these gross physical and mechanical differences between mouse intervertebral segments would be associated with inherent material and structural variations at the histological level. Our hypothesis does not preclude the possibility that key microscopic features may be conserved among non-degenerated IVD from thoracic, lumbar, sacral, and caudal levels (Tam et al., 2018).

2 | MATERIALS AND METHODS

2.1 | Animals and tissue sampling

Vertebral columns were obtained from male C57BL/6N and C57BL/6JRj mice at the following time points: 4 weeks (weaned, both stains, C57BL/6N: $n = 7$; C57BL/6JRj: $n = 4$), 3 months (mature, both stains, C57BL/6N: $n = 7$; C57BL/6JRj: $n = 4$), 12 months (middle aged, C57BL/6JRj only, $n = 3$), and 18 months (old, C57BL/6JRj only, $n = 3$; Dutta & Sengupta, 2016; Flurkey et al., 2007). In addition, knee joints were obtained from mature mice for comparison of cartilage-like staining in the vertebral sections. Prior to dissection, the mice were sacrificed by asphyxiation with carbon dioxide (CO_2). All procedures followed the European guidelines on animal welfare and experiments (directive 2010/63/EU) and were approved by the local governmental animal care and use committee (Landesdirektion Sachsen, application number T21/18). The body cavities of dead mice were opened and the organs removed, using dissection scissors and forceps. The vertebral column was carefully and thoroughly freed from surrounding muscle tissue and removed caudal to the thoracic level. The vertebral column was further divided into lumbar (Th13 to S1) and tail (C2-C10) segments to fit into embedding cassettes. To obtain an impression of the gross morphological differences between lumbar and tail discs, individual discs were isolated from animals of different ages. For these macroscopic analyses, the IVD were separated as closely as possible to the distal superior and proximal inferior vertebral body endplates using a microtome knife. Special attention was paid to avoid injury of the annuli fibrosi during the dissection and isolation process. All specimens (vertebra segments/ knee joints), intended for histological sectioning and evaluation, were fixed in 4% buffered formalin (pH 7.4) for several hours at 4°C then transferred to a decalcification solution of 0.5 M ethylenediaminetetraacetic acid (EDTA, pH8, Avantor VWR International GmbH) until the bony portions of the specimens were completely decalcified. This was achieved in 4–5 days at 4°C. Isolated individual discs were fixed then embedded in paraffin directly and used for photo documentation. Histological analysis of the surgical removed, embedded and sectioned vertebral segments comprised the intervertebral disc segments between Th13/S1 and C2/C10.
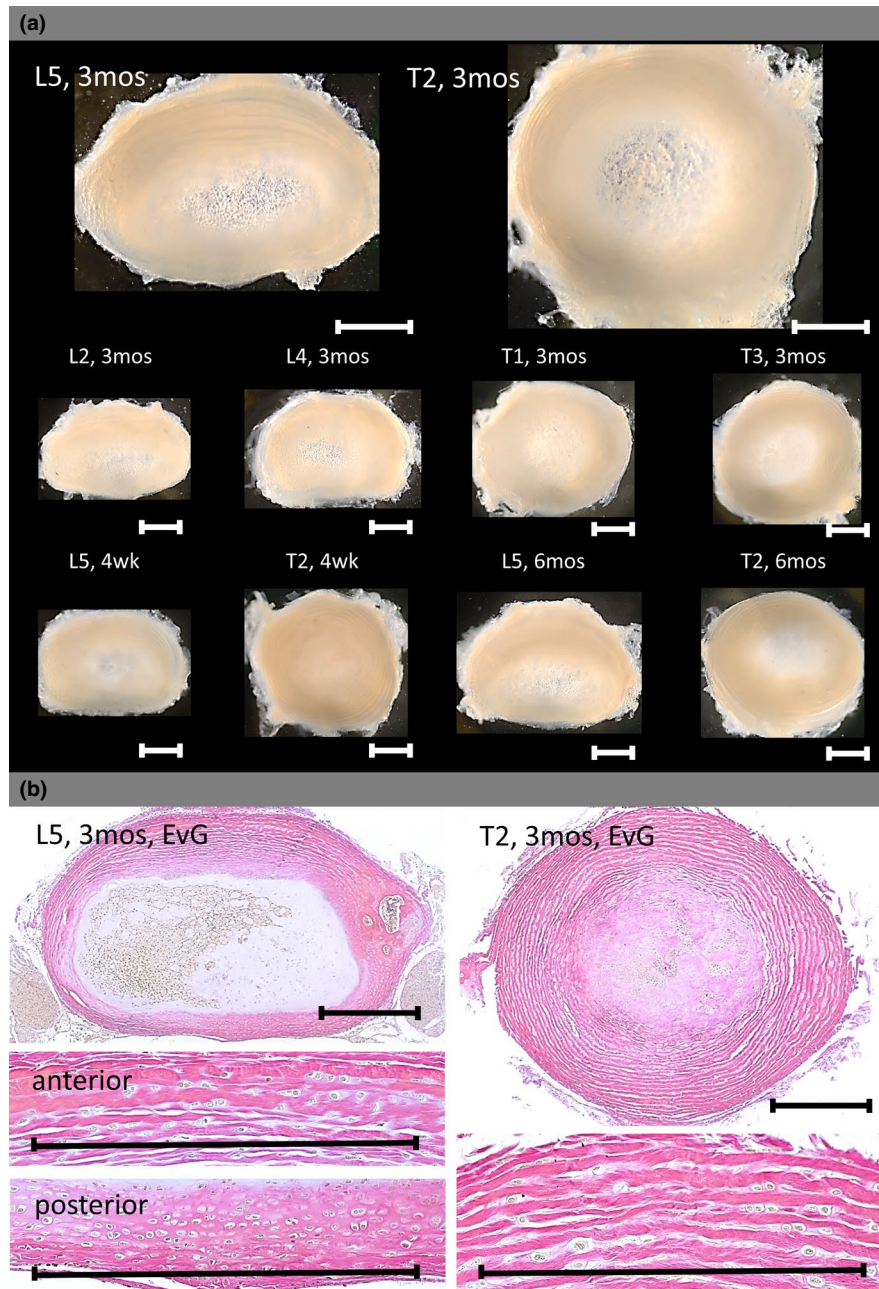
FIGURE 1 (a) Transverse view of intervertebral discs (IVD) from the lumbar (L) and tail (T) levels of 4-week, 3-month and 6 months old C57BL/6N mice. Comparing the IVD at the two levels, differences in shape, nuclei pulposi position (NP), and distinctness of annuli fibrosus lamellae can be appreciated, irrespective of age. Lumbar IVD are elliptical to kidney-shaped regardless of their location, with slightly dorsally located nuclei pulposi. The annuli fibrosus of lumbar IVD contain broad and easily identifiable lamellae only in the ventral and lateral aspects. Dorsally, individual lamellae of lumbar IVD are thin, tightly packed, and difficult to distinguish. In contrast, the tail IVD are rounded in shape, regardless of their location, and their NP are located centrally. The lamellae of the AF in tail IVD are broad and easily identifiable around their entire circumference. (b) Elastica van Gieson (EvG) staining of a transverse-sectioned IVD demonstrating that, compared to lumbar IVD, tail IVD contain more organized collagen bundles and cells that form circumferentially distinct AF lamellae. Scale bar equals 0.5 mm

2.2 | Intervertebral disc gross morphology

To provide an impression of disc gross morphological differences between lumbar and tail discs, individual discs were examined and photodocumented with an Olympus SZ61 stereomicroscope equipped with a digital SC30 camera and laptop running cellSens image acquisition software (all Olympus).

2.3 | Histological sections and stains

Fixed and decalcified vertebral column segments were dehydrated in a graded series of alcohol before being paraffin-embedded in the coronal plane. The embedded segments were serially sectioned into 10 μm thick slices and mounted onto glass slides. Individual paraffin sections were deparaffinized by running them through xylene,

alcohol, and water. Hematoxylin-eosin and bone and cartilage staining techniques were carried out according to the standard protocols described in detail in Romeis Mikroskopische Technik (19th edition) (Mulisch & Welsch, 2015). Alcian blue was used to stain cartilage and Light green was used to stain bone. Goldner's Masson's and Azan trichrome stains were used to stain both bone and cartilage. Elastica van Gieson and Weigert's Resorcin Fuchsin stain were used to stain collagen and elastin, respectively. After staining, the slides were rinsed, dehydrated in alcohol, cleared in xylene, and covered with a coverslip. The slides were then evaluated under an Axioplan 2 upright light microscope (Zeiss), photographed with a ProgRes C3 digital camera (Jenoptik), and documented with a digital recording system (ProgRes CapturePro 2.8.8; Jenoptik).

3 | RESULTS

No significant differences in the histology of any structural component of the IVD, including nucleus pulposus, annulus fibrosus, and endplate, were observed when comparing the two C57BL/6 mouse strains at ages 4 weeks and 3 months. Therefore, no further distinction was made between the mouse strains when describing study findings.

3.1 | Gross morphology of lumbar and tail IVD of the mature mouse

Both lumbar and tail discs of mature mice appeared as white and mildly convex structures (Figure 1). Tail discs were almost round in the transverse plane, while lumbar discs were oval or kidney-shaped. The overall height and the transverse cross-sectional area were greater for all tail discs compared to any lumbar disc. The annulus fibrosus (AF) of al tail discs was of uniform thickness at all points along the disc circumference. Its lamellae were easily identifiable in all areas. In contrast, the AF of lumbar discs showed variations in thickness around their circumferences. In all lumbar discs the AF were thicker in the ventral and lateral areas compared to the dorsal area. Similarly, the lamellae were more readily identifiable in the ventral and lateral areas than in the dorsal area, were the lamellae were thin, tightly packed, and difficult to discern as individual units. The central amorphous nucleus pulposus (NP) of both lumbar and tail discs was similarly milky in appearance and of soft consistency.

3.2 | Comparison of lumbar and tail IVD histology

Lumbar and tail IVD regions consisted of four major structures: an inner NP, an outer AF, and superior and inferior endplates (EP). The EP linked the other IVD components to the cartilagenous growth plates of trabecular bone at either end of the vertebral bodies. No significant morphological differences were observed between the superior and inferior EP of the same vertebral unit in adult mice.

However, the EP of lumbar and tail vertebra demonstrated significant differences (Figure 2).

Lumbar superior and inferior EP were primarily cartilagenous EP (Figure 2a,c, CEP), composed of hyaline cartilage with several layers of chondrocytes. Bony material was absent or was restricted to small secondary ossification centers. The CEP and the AF merged into each other and appeared as a homogeneously-stained structure in the majority of the histological staining procedures. In contrast to the lumbar EP, tail superior and inferior EP were primarily bony (Figure 2b,d, BEP). A small rim of one to three cartilaginous endplate cell (CEC) layers at the border of the NP abutted subchondral bone (SCB), which appeared as a robust structure with broad secondary ossification centers and multiple vascular channels. Of note, axial herniation of disc tissue, that is, occasional disruptions along the EP, resembling Schmorl's nodes (Figure 2a,b, asterisks¸ DOI: Adams & Dolan, 2012; Moore, 2006), were occasionally observed at both vertebral levels. Growth plate cartilages (GPC) joining the EP to TB were evident at both vertebral levels (Figure 2c,d). The NP at the center of both the lumbar and tail discs consisted of a peripheral space filled with a loosely structured amorphous mass (AM) and a central cluster of vacuolated interconnected cells (VIC) (Figure 2e,f). The cells were predominantly of the typical notochordal cell type with a single giant cytoplasmic vacuole, with fewer of the smaller chondrocytic eosinophilic cell type. In coronal sections of lumbar IVD, the central VIC were mainly arranged in a single cluster with an elliptical, "cigar-like" appearance (Figure 2a,e). In contrast, in coronal sections of tail IVD, there was evidence of further organization beyond the level of the single cluster, with the appearance of multiple subclusters. The subclusters were loosely organized, giving the entire cluster an overall appearance of an "aster" (Figure 2b,f). The AF of both lumbar and tail discs showed distinct robe-like fiber structures with characteristic banding. However, the AF of tail discs were significantly thicker and their concentric lamellae more pronounced when compared to those of lumbar discs (not shown).

3.3 | Comparison of connective tissue staining in IVD and knee joints

The EP at both the lumbar and tail level exhibited staining characteristics comparable with subchondral/trabecular bone (SCB/TB) and tibial articular hyaline cartilage (AHC) of the synovial knee joint, regardless of the staining procedure used (Figure 3). The only exception to this staining pattern was noted in Alcian blue-stained sections. Here, the CEP of lumbar discs stained similarly to GPC of the vertebral body and the proximal tibia. In contrast, the EP of tail discs exhibited characteristics similar to the bony parts of vertebral bodies and tibiae.

3.4 | Age-related changes in lumbar and tail IVD histology

In weaned 4-week-old mice, regardless of the C57BL6 substrain (Figure 4, upper four rows), the EP differences between lumbar
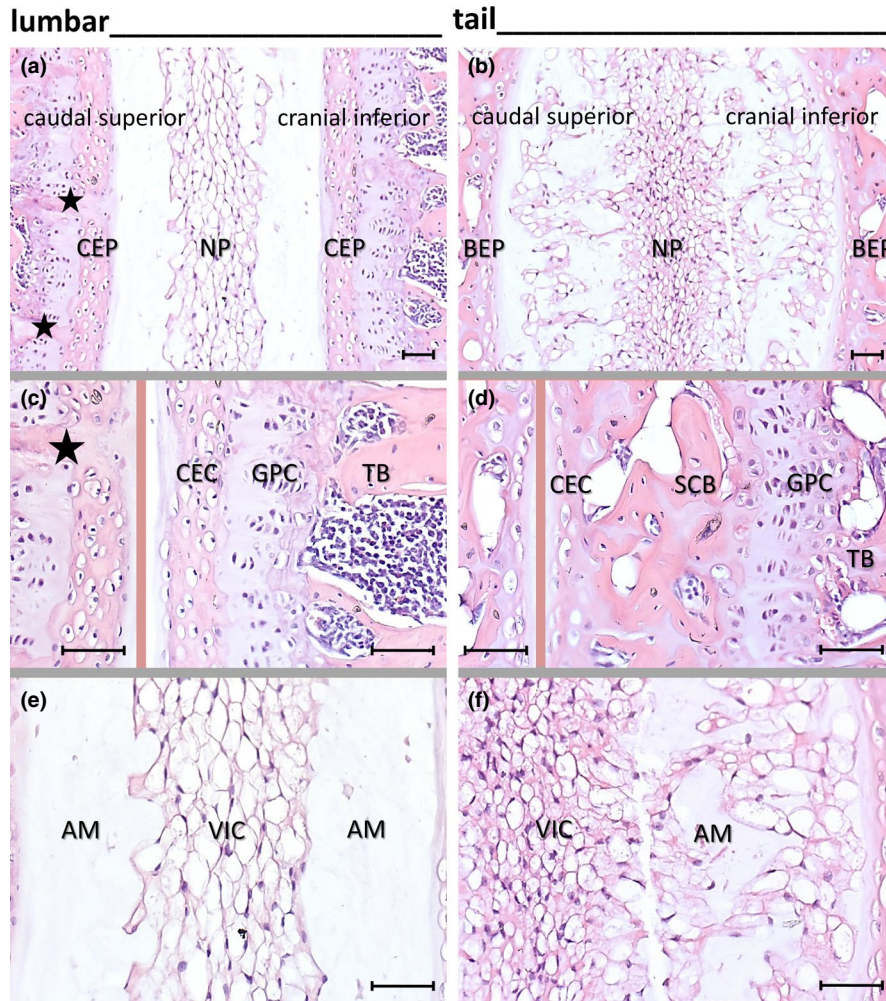
FIGURE 2 Representative mid-coronal hematoxylin and eosin-stained sections of lumbar (left column) and tail (right column) intervertebral disc (IVD) endplate segments of a mature (3 months old) male C57BL/6N mouse. Low-power (a and b) and high-power field views (c–f). The low power field views depict the nuclei pulposi (NP) and the adjacent cartilaginous (CEP) and bony endplates (BEP). (c) The CEP in the lumbar segment consists of several layers of cartilaginous endplate cells (CEC) directly abutting the vertebral growth plate cartilage (GPC) and trabecular bone (TB). The stars in (a and c) mark protrusions of the disc tissue through the EP, resembling Schmorl's nodes. (d) The BEP in the tail segment contains one to two rows of CEC first followed by subchondral bone (SCB) adjacent to growth plate cartilage and trabecular bone. Broad secondary ossification centers and vascular channels are readily apparent in the SCB. (e and f) show the NP of two segments at higher magnification. (e) The lumbar NP contains a well-defined central cluster of vacuolated interconnected cells (VIC), sharply demarcated from a peripheral VIC-free, poorly organized amorphous mass (AM). (f) In tail discs, the main central cluster of VIC is interconnected to multiple subclusters of VIC in the poorly organized AM in the periphery. AM, amorphous mass; BEP, bony endplate; CEC, cartilaginous endplate cells; CEP, cartilaginous endplate; GPC, growth plate cartilage; NP, nucleus pulposus; SCB: subchondral bone; TB, trabecular bone; VIC, vacuolated interconnected cells. Scale bar equals 50 µm in each photograph

and tail IVD described above were even more pronounced than in 3 months old or mature mice. Surprisingly, the observed morphological differences between lumbar and tail EP persisted and were still visible in middle age and old C57BL/6JRj mice (Figure 4, lower four rows). However, the organization and structure of lumbar EP progressively approximated to those of the tail with increasing age. By comparing older mice to weaned and 3 months old mice histological tissue changes in the EP included a transition toward smaller, less polygonal cartilage cells and broader secondary ossification centers and vascular channels. These changes occurred both in the cranial inferior and caudal superior EP, although they were found more frequently in the cranial inferior than the caudal superior endplate. Conspicuous changes in the structure of the NP also occurred in both vertebral segments. The relative size of the amorphous mass was noticeably larger in the IVD of older mice compared to weaned and 3-month-old animals. Small non-vacuolated eosinophilic cells now prevailed over large uni-vacuolated cells in the cellular clusters, which were confined to the NP centers now at both vertebral levels. The age-related changes in the NP were more prominent in lumbar compared to tail IVD segments.
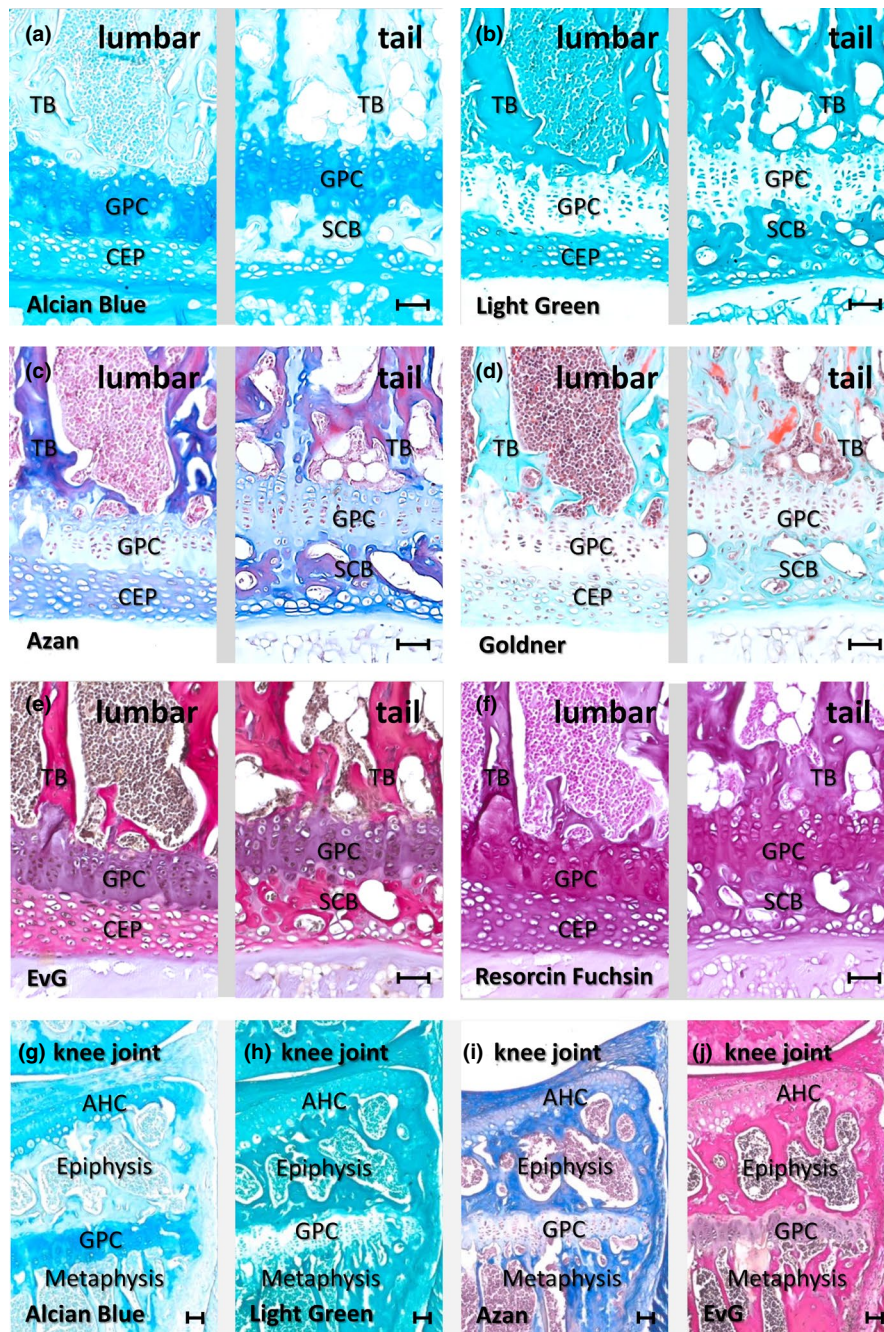
FIGURE 3 (a–g) Mid-coronal histological sections of lumbar and tail intervertebral disc (IVD) endplate segments of a mature (3 months old) male C57BL76N mouse. (a and b) show sections stained for cartilage and bone using Alcian blue and Light green, respectively. (c and d) display sections stained with classical histological stains [Azan (c), Goldner Trichrome (d)] for cartilage and bone. (d and e) demonstrate sections with connective tissue stains [Elastica van Gieson (e, EvG), Weigert's Resorcin Fuchsin (f)]. Under most staining conditions, the lumbar cartilaginous endplate (CEP) shows characteristics similar to those of articular hyaline cartilage and subchondral (SCB) or trabecular bone (b). Only Alcian blue results in a CEP staining pattern more similar to that of growth plate cartilage (GPC). (g–j) Comparative images of Alcian blue (g), Light green (h), Azan (i), and EvG stained (j) sections of knee joints from 3 months old mice. The tibial hyaline articular cartilage (AC) shows a similar staining pattern to the CEP of the vertebra bodies above. AHC, articular hyaline cartilage; CEP, cartilaginous endplate; GPC, growth plate cartilage; TB, trabecular bone; SCB, subchondral bone. Scale bar equals 50 μm in each photograph

4 | DISCUSSION

In this study, we highlight significant differences in the histological features between lumbar and tail IVD in mice. We believe that our findings are likely to reflect distinct mechanical properties between these two-disc levels of the spine during life and that histologic IVD heterogeneity also explains differences in energy metabolism, nutrient supply, and production of matrix components (Elliott & Sarver, 2004; Sarver & Elliott, 2005).
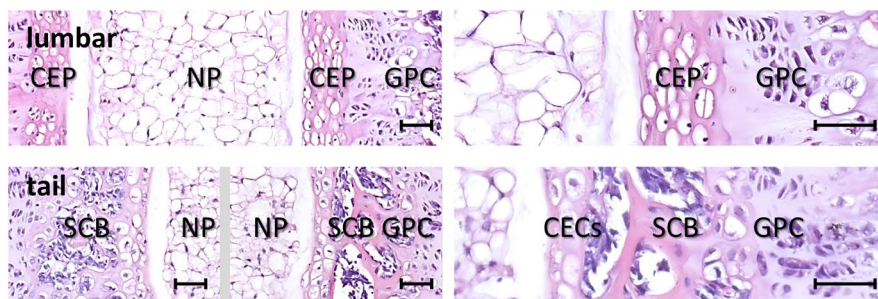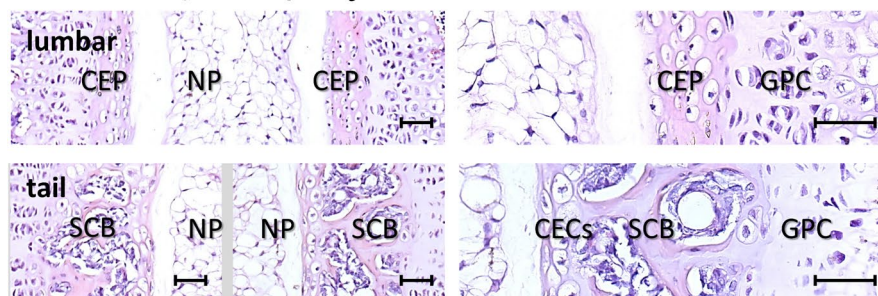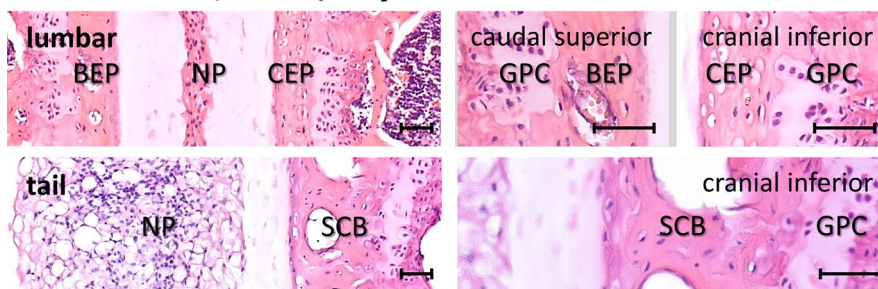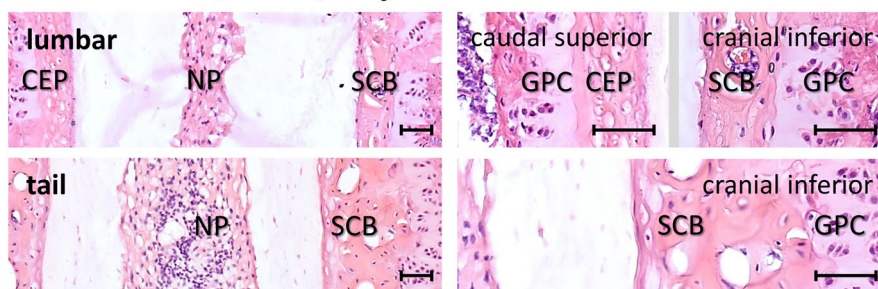
FIGURE 4 Mid-coronal histological sections of lumbar and tail intervertebral disc (IVD) segments from animals of different ages. The IVD endplate segments of 4 weeks old C57BL/6N and C557BL/6JRj mice display similar histological features as observed in the lumbar endplate segments of 3 months old C57BL/6N mice. At 4 weeks, the cartilaginous organization of the lumbar endplate is even more distinct than at 3 months of age (see Figure 2 for comparison) and clearly differs in bony organization compared to the bony endplate of tail IVD. Interconnected large vacuolated cells almost entirely occupy the nuclei pulposi of both IVD segments. Only a thin rim of loosely structured amorphous mass occupies the outermost of the periphery. At ages 12 and 18 months, the morphological organization of the lumbar endplate starts to resemble that in tail IVD-segments. The changes range from smaller, less polygonal cells to secondary ossification centers and vascular channels. The changes occur in both cranial inferior and caudal superior endplates but are observed more commonly in the cranial inferior endplate. In comparison with the younger ages, the nuclei pulposi in both vertebral segments show a tremendous increase in the loosely structured amorphous mass, a localization of cellular elements to the disc center, and replacement of the large vacuolated cells by small non-vacuolated eosinophilic cells. Of note, at both vertebral levels, growth plate cartilage (GCP) is still visible in the endplate-vertebral body interface. BEP, bony endplate; CEP, cartilaginous endplate; GPC, growth plate cartilage; NP, nucleus pulposus; SCB, subchondral bone; TB, trabecular bone. Scale bar equals 50 μm in each photograph

Although IVD histology requires dissecting and sectioning which ultimately destroys the three-dimensional (3D) anatomy of IVD, and may introduce artifactual spacial distortion, the method still affords high resolution and precise evaluation of IVD tissue (Bhalla et al., 2017; Cao et al., 2017; Tam et al., 2018). It is of note, that we consistently examined midcoronal sections of IVD in lumbar and tail vertebrae. Studies by others have verified that sagittal/coronal sections exhibit consistency in key structural features of IVD and, therefore, vertebral sections from either plane can be used if the method of preparation is consistent (Tam et al., 2018).

The histology of all three major compartments of mouse IVD, that is, NP, AF, and EP varied significantly between lumbar and tail discs throughout development and maturation. In mature animals, NP differed in the arrangement of central interconnected single vacuolated cells. The central cluster of single vacuolated cells in lumbar NP was compact and restricted to the middle of the NP. In tail NP, the cluster was divided into subclusters, which extended into the amorphous extracellular matrix at the NP peripheries. At all developmental stages, the AF of tail discs were thicker than those of lumbar discs.

Substantial differences existed between the lumbar and tail IVD-EP-interphases in mature mice. At this stage, the lumbar IVD-EP-interphase appeared as a broad CEP in continuum with the GP cartilage of the vertebral body. In contrast, the tail endplates were remarkable for a broad bony layer adjacent to the GPC of the vertebral body with only a few rows of cartilage cells intervening between the bony layer and the NP/AF. The GPC in lumbar and tail vertebral bodies was easily identifiable and composed of chondrocyte columns with dividing cells and persisted up to old age.

The finding of different EP morphologies in lumbar and tail IVD-EP-interphases in adult mice might be important in several aspects. Firstly, the findings provide a further structural explanation for the reported biomechanical differences, between lumbar and tail discs in mature mice (Elliott & Sarver, 2004; Melrose et al., 1994; Sarver & Elliott, 2005). Secondly, given that nutrients must diffuse across the EP to reach the avascular NP and AF, variations in EP morphology, particularly the degree of ossification, may be critical in determining EP transport properties. Finally, as EP are the main site of changes in IDD, variations in EP ossification may modify the susceptibility to and evolution of IDD (Laffosse et al., 2010; Moore, 2000).

It is important to note that neither the lumbar nor the tail IVD-EP-interphase in mice recapitulates the histology of the adult human IVD-EP-interphase (Tam et al., 2018). However, since calcification of human endplates begins around the age of 6, and ossification is complete by age 13, the lumbar and tail IVD-EP-interphase could be considered histologically representative of infant cartilaginous and juvenile bony IVD-EP-interphases, respectively.

GP are absent in adult human vertebral bodies. Adult human EP contain a thick cartilaginous zone near the IVD and a secondary bony zone abutting the primary trabecular bony zone of the vertebral body (Zhang et al., 2014). The cartilaginous zone most likely consists of partly calcified fibrocartilage with only scant cells. The bony zone contains relatively few vascular channels. The NP in human lumbar discs is primarily fibrous. Adult human NP may still contain small notochord cell remnants, but the majority of the notochord-like vacuolated cells disappear rapidly after birth, which may have implications for regenerative potential (Alini et al., 2008; Oegema Jr., 2002; Yu et al., 1989).

The staining of EP cartilage in mouse IVD-EP-interphases differed from that of GP cartilage, being similar to hyaline articular cartilage of the knee joint. This is in line with observations in humans, where the proteoglycan and collagen composition of EP cartilage seems to be more akin to articular than epiphyseal cartilage (Roberts et al., 1989).

One major challenge that confounds the study of IVD morphology is that IVD are subject to age-related changes (Pattappa et al., 2012). The structure of the NP may vary significantly with disc maturity in some species (Hunter et al., 2004). Therefore, it was of great interest to compare IVD specimens from weaned, mature, middle aged and older mice to understand the evolution of NP and GP structure within this species. We found that the NP cells in mice changed from notochord-like vacuolated to non-vacuolated cells with the progression of age. However, vacuolated NP cells were still present into old age which is in accordance with existing literature (Alini et al., 2008; Bhalla et al., 2017; Dahia et al., 2009). This may enable mouse IVD to stay healthy and equip them with a greater regenerative potential than human discs (Alini et al., 2008; Bhalla et al., 2017; Oegema Jr., 2002). Furthermore, since GP were present in mice up to the age of one-and-a-half years, it is doubtful that sex hormones play a major role in growth plate closure and resultant termination of longitudinal vertebral growth in this animal. This finding underscores the observation that sexually mature and even-aged mice still have the potential for longitudinal growth (Flurkey et al., 2007; Zhang et al., 2014). It is of particular interest, that the above-described differences between lumbar and tail IVD-EP-segments could still be partly observed in 18 month-old mice. It is unclear whether these level-specific histological differences in mouse EP and NP result from functional adaptions of the vertebral column that have evolved to permit different corporal movements and/or withstand different mechanical loading conditions (Alini et al., 2008). When comparing lumbar and tail IVD-segments, tail IVD-segments appeared more mature than lumbar IVD-segments in terms of NP- and EP-morphologies. We observed that NP of tail discs in adult mice had dispersed notochordal cells with an accumulated amorphous matrix and bony EP, which are indicative of a more advanced maturational process. Development of these features in NP may be potentiated by greater mechanical stress and reduced nutrition supply upon calcification of the EP.

Our study reveals that, in the same animal, EP cartilage exists either in direct continuation with GP cartilage (cartilaginous EP) or separated from GP cartilage by a bony layer (bony EP). Our study demonstrates that, contrary to previous assumptions, the mouse has bony EP as well as cartilaginous EP (Dahia et al., 2009; Zhang et al., 2014). Our data indicate that histological EP differences are more disc level than species-specific (Zhang et al., 2014). We, therefore, suggest that disc level-dependent peculiarities should be considered

when mice are used as animal models for the study of IDD and its surgical management. The remarkable morphological differences between lumbar and tail IVD in mice provide a unique opportunity to study level-specific development, biomechanics, and nutritional supply under controlled conditions.

4.1 | Conclusion

We have clearly demonstrated that mice possess spinal level and age-dependent bony EP as well as unossified cartilaginous EP. Previously reported level-dependent differences in the biomechanical and biochemical properties of IVD in mice are likely to be functional correlates of the significant histological heterogeneity observed in our analyses. Although rodent tail discs may serve as useful models for IVD research, caution is necessary when extrapolating data obtained in tail discs to lumbar discs and vice versa. Our findings are of relevance to biomedical researchers seeking to use mouse models for the study of human IVD disorders and their treatment.

AUTHOR CONTRIBUTIONS

JB and AMR designed the study and assembled the data. AMR drafted the manuscript. AS critically interpreted the data and wrote the final version of the manuscript together with AMR and PL. KW was heavily involved in morphological data acquisition, analysis, and interpretation. All authors critically revised and approved the final manuscript version.

DATA AVAILABILITY STATEMENT

The data that support the findings of this study are available on reasonable request by email addressed to the corresponding author (AMR).

ORCID

Albert Markus Ricken https://orcid.org/0000-0003-1616-6964

REFERENCES

Adams, M.A. & Dolan, P. (2012) Intervertebral disc degeneration: evidence for two distinct phenotypes. *Journal of Anatomy*, 221, 497–506.

Alini, M., Eisenstein, S.M., Ito, K., Little, C., Kettler, A.A., Masuda, K. et al. (2008) Are animal models useful for studying human disc disorders/degeneration? *European Spine Journal: Official Publication of the European Spine Society, the European Spinal Deformity Society, and the European Section of the Cervical Spine Research Society*, 17, 2–19.

Bhalla, S., Lin, K.H. & Tang, S.Y. (2017) Postnatal development of the murine notochord remnants quantified by high-resolution contrast-enhanced MicroCT. *Scientific Reports*, 7, 13361.

Boszczyk, B.M., Boszczyk, A.A. & Putz, R. (2001) Comparative and functional anatomy of the mammalian lumbar spine. *The Anatomical Record*, 264, 157–168.

Cao, Y., Liao, S., Zeng, H., Ni, S., Tintani, F., Hao, Y. et al. (2017) 3D characterization of morphological changes in the intervertebral disc and endplate during aging: a propagation phase contrast synchrotron micro-tomography study. *Scientific Reports*, 7, 43094.

Dahia, C.L., Mahoney, E.J., Durrani, A.A. & Wylie, C. (2009) Postnatal growth, differentiation, and aging of the mouse intervertebral disc. *Spine*, 34, 447–455.

Daly, C., Ghosh, P., Jenkin, G., Oehme, D., Goldschlager, T. & Gualillo, O. (2016) A review of animal models of intervertebral disc degeneration: pathophysiology, regeneration, and translation to the clinic. *BioMed Research International*, 2016, 5952165. https://doi.org/10.1155/2016/5952165

Dutta, S. & Sengupta, P. (2016) Men and mice: relating their ages. *Life Sciences*, 152, 244–248.

Elliott, D.M. & Sarver, J.J. (2004) Young investigator award winner: validation of the mouse and rat disc as mechanical models of the human lumbar disc. *Spine*, 29, 713–722.

Flurkey, K., Currer, J.M. & Harrison, D.E. (2007) Mouse models in aging research. In: Fox, J.G., Davisson, M.T., Quimby, F.W., Barthold, S.W., Newcomer, C.E. & Smith, A.L. (Eds.) *The mouse in biomedical research*. Amsterdam: Elsevier Academic Press, pp. 637–672.

Holguin, N., Aguilar, R., Harland, R.A., Bomar, B.A. & Silva, M.J. (2014) The aging mouse partially models the aging human spine: lumbar and coccygeal disc height, composition, mechanical properties, and Wnt signaling in young and old mice. *Journal of Applied Physiology (Bethesda, MD: 1985)*, 116, 1551–1560.

Hunter, C.J., Matyas, J.R. & Duncan, N.A. (2004) Cytomorphology of notochordal and chondrocytic cells from the nucleus pulposus: a species comparison. *Journal of Anatomy*, 205, 357–362.

Laffosse, J.-M., Kinkpe, C., Gomez-Brouchet, A., Accadbled, F., Viguier, E., Sales de Gauzy, J. et al. (2010) Micro-computed tomography study of the subchondral bone of the vertebral endplates in a porcine model: correlations with histomorphometric parameters. *Surgical and Radiologic Anatomy: SRA*, 32, 335–341.

McCann, M.R. & Séguin, C.A. (2016) Notochord cells in intervertebral disc development and degeneration. *Journal of Developmental Biology*, 4, 3. https://doi.org/10.3390/jdb4010003

Melrose, J., Ghosh, P., Taylor, T.K.F. & McAuley, L. (1994) A comparative study of the composition of discs and of proteoglycans from different spinal levels of sheep. *Veterinary and Comparative Orthopaedics and Traumatology*, 7, 70–76.

Moore, R.J. (2000) The vertebral end-plate: what do we know? *European Spine Journal: Official Publication of the European Spine Society, the European Spinal Deformity Society, and the European Section of the Cervical Spine Research Society*, 9, 92–96.

Moore, R.J. (2006). The vertebral endplate: disc degeneration, disc regeneration. *European Spine Journal*, 15(S3), 333–337. https://doi.org/10.1007/s00586-006-0170-4

Mulisch, M. & Welsch, U. (2015) *Romeis - Mikroskopische Technik*. Berlin, Heidelberg: Springer Berlin Heidelberg.

O'Connell, G.D., Vresilovic, E.J. & Elliott, D.M. (2007) Comparison of animals used in disc research to human lumbar disc geometry. *Spine*, 32, 328–333.

Oegema Jr., T.R. (2002) The role of disc cell heterogeneity in determining disc biochemistry: a speculation. *Biochemical Society Transactions*, 30, 839–844.

Pattappa, G., Li, Z., Peroglio, M., Wismer, N., Alini, M. & Grad, S. (2012) Diversity of intervertebral disc cells: phenotype and function. *Journal of Anatomy*, 221, 480–496.

Roberts, S., Menage, J. & Urban, J.P. (1989) Biochemical and structural properties of the cartilage end-plate and its relation to the intervertebral disc. *Spine*, 14, 166–174.

Sarver, J.J. & Elliott, D.M. (2005) Mechanical differences between lumbar and tail discs in the mouse. *Journal of Orthopaedic Research: Official Publication of the Orthopaedic Research Society*, 23, 150–155.

Tam, V., Chan, W.C.W., Leung, V.Y.L., Cheah, K.S.E., Cheung, K.M.C., Sakai, D. et al. (2018) Histological and reference system for the analysis of mouse intervertebral disc. *Journal of Orthopaedic Research: Official Publication of the Orthopaedic Research Society*, 36, 233–243.

Yu, S.W., Haughton, V.M., Lynch, K.L., Ho, K.C. & Sether, L.A. (1989) Fibrous structure in the intervertebral disk: correlation of MR appearance with anatomic sections. *AJNR: American Journal of Neuroradiology*, 10, 1105–1110.

Zhang, Y., Lenart, B.A., Lee, J.K., Chen, D., Shi, P., Ren, J. et al. (2014) Histological features of endplates of the mammalian spine: from mice to men. *Spine*, 39, E312–E317.